J Mater Sci (2015) 50:5571–5577
DOI 10.1007/s10853-015-9104-z

Bright red-emitting polymer dots for specific cellular imaging

Wei Zhang[1] · Hang Sun[3] · Shengyan Yin[2] · Jingjing Chang[1] · Yanhui Li[1] · Xingyuan Guo[2] · Zhen Yuan[4]

Received: 10 March 2015 / Accepted: 14 May 2015 / Published online: 20 May 2015

Abstract A new conjugated polymer, poly[{2-methoxy-5-(2-ethylhexyloxy)-1,4-(1-cyanovinylphenylene)}-alt-co-{2,5-bis(*N*,*N*′-diphenylamino)-1,4-phenylene}] (DB-CN-PPV), with strong UV absorption and high fluorescence in red wavelength region, is self-assembled into nanoparticles (polymer dots, Pdots) in aqueous solution upon rapid mixing of the organic solution with water. Different-sized Pdots were obtained by varying the organic solvent percent in the mixture solution and further characterized by dynamic light scattering and transmission electron microscopy. Spectroscopic measurements indicate that the DB-CN-PPV Pdots exhibit a bright red-emitting and a quantum yield of ~27 %. Single-particle imaging and analyses indicate the brightness of DB-CN-PPV Pdots under 405 nm excitation is four times brighter than that of the well-known inorganic quantum dot probes, Qdot655, under same excitation light. The successful bioconjugation and cellular imaging suggest DB-CN-PPV Pdots have potential application for biological fluorescence imaging.

✉ Shengyan Yin
syyin@jlu.edu.cn

✉ Yanhui Li
liyanhui@ciac.ac.cn

[1] School of Materials Science and Engineering, Changchun University of Science and Technology, Changchun 130022, Jilin, People's Republic of China

[2] State Key Laboratory on Integrated Optoelectronics, College of Electronic Science Engineering, Jilin University, Changchun 130012, Jilin, People's Republic of China

[3] Key Laboratory of Bionic Engineering (Ministry of Education), College of Biological and Agricultural Engineering, Jilin University, Changchun 130022, Jilin, People's Republic of China

[4] Bioimaging Core, Faculty of Health Science, University of Macau, Taipa, Macau SAR, People's Republic of China

Introduction

In the past decade, the development of fluorescence spectroscopy and microscopy combined with bioconjugation techniques is leading to a rapid proliferation of advanced fluorescence-based applications in chemistry and biomedical sciences [1, 2]. A bunch of fluorescent probes have been adopted and implemented for diverse cell imaging and tracing, such as fluorescent proteins, organic dyes, and inorganic quantum dots (Qdots) [3–8]. However, for long-term imaging and sensing, the performance of fluorescent proteins and organic dyes are significantly affected by their low photo-bleaching threshold. For example, although silica or polymer coating technique has promoted the colloidal stability of Qdots, the heavy metal ions present in Qdots would generate toxic effect on living organisms or biological cells [9–12]. Interestingly, semiconducting polymer dots (Pdots), as a new kind of nanomaterials with excellent photostability and low biological toxicity, have shown its promise in cell imaging, drug delivery and release, and disease diagnosis [1, 13, 14]. Importantly, the Pdots has been extensively investigated in different perspectives including preparation and preparation methods [15–17], extraordinary florescence brightness [18], nontoxic features [19], high-speed single-particle tracking [20], biocompatibility [1], and photostability [16]. In particular, Pdots with different luminescent wavelengths have been reported successfully. To date, the major technique challenges that lie ahead of us for the development of Pdots is to design and synthesis a high fluorescence probe in red wavelength range since red

wavelength region is more useful for the analysis of biological systems [21].

Recently, polyphenylene vinylene (PPV) and their derivatives as promising electroluminescent materials have received considerable attention in organic light-emitting diode, light pumped laser, field effect transistor, and organic photovoltaic cell [22]. Due to their unique luminescent properties, these derivatives have been utilized to formulate the fluorescent polymer, such as MEH-PPV [17, 23], MDMO-PPV [24], and CN-PPV [13], which will extend its biomedical applications. In this study, we report a novel Pdots species based on a PPV derivative, Poly[{2-methoxy-5-(2-ethylhexyloxy)-1,4-(1-cyanovinylphenylene)}-alt-co-{2,5-bis(*N*,*N*′diphenylamino)-1,4-phenylene}] (DB-CN-PPV). These DB-CN-PPV Pdots, when formed by reprecipitation, are more compact and smaller in size with an average hydrodynamic diameter of ~20 nm; they also exhibit a higher red fluorescence with a quantum yield ~27 %. We also utilize the polymer conformation in solution phase to control the polymer folding and packing during the nanoparticle preparation process, and obtain different-sized Pdots. In addition, the emission peak can be adjusted while mixed with poly [(9,9-dioctylfluorenyl-2,7-diyl)-co-(1,4-benzo-{2,1,3}-thiadiaole)] (PFBT). Further, single-particle imaging was performed, which indicated that these Pdots show better brightness compared that from Qdots. Successful functionalization and bioconjugation were conducted, which produces DB-CN-PPV-streptavidin bioconjugates that are able to specifically label cell-surface markers and sub-cellular microtubule structures in mammalian cells. This investigation will not only provide a promising way for further developing functional Pdots for cellular imaging, but also present a new kind probe of bioanalytical assays.

Materials and methods

Materials

The conjugated polymers employed in this study are the PPV derivative Poly[{2-methoxy-5-(2-ethylhexyloxy)-1,4-(1-cyanovinylphenylene)}-alt-co-{2,5-bis(*N*,*N*′-diphenylamino)-1,4-phenylene}] (DB-CN-PPV; average MW 19,000, polydispersity 2.7) and polyfluorene derivative poly[(9,9-dioctylfluorenyl-2,7-diyl)-co-(1,4-benzo-{2,1,3}-thiadiaole)] (PFBT; average MW 157,000, polydispersity 3.0), which were purchased from ADS Dyes, Inc. (Quebec, Canada). The functional copolymer poly (styrene-co-maleic anhydride) (PSMA, cumene terminated, average Mn ~1700, styrene content 68 %), the solvent Tetrahydrofuran (THF, anhydrous, ≥99.9 %), and streptavidin were purchased from Sigma-Aldrich. 1-ethyl-3-(3-dimethylaminopropyl) carbodiimide (EDC) was purchased from Thermo Fisher Scientific (Rockford, IL, U.S.A). Qdots655 was purchased from Invitrogen of America. The solvent ethanol (analytical reagent, ≥99.7 %) was purchased from Beijing Chemical Works (Beijing, China). All chemicals were used without further purification and all experiments were performed at room temperature unless indicated otherwise. Breast cancer cell line MCF-7 cells were ordered from Shanghai Fuxiang Biotechnology Co. Ltd. (Shanghai, China).

Preparation of semiconducting polymer nanoparticles

Semiconducting Pdots were prepared by the modified reprecipitation method [25]. Briefly, the semiconducting polymer DB-CN-PPV and functional polymer PSMA were dissolved in pure THF to prepare a stock solution with a concentration of 1 mg/mL, respectively. And then two polymer solutions were mixed in pure THF with a DB-CN-PPV concentration of 50 μg/mL and a PSMA concentration of 10 μg/mL. We used this mixture solution as the starting organic solution. Secondly, a 5 mL of the above starting organic solution quickly injected into 10 mL of Milli-Q water in bath sonicator. The sudden decrease in solvent quality results in nanoparticle formation. Finally, the solvent THF was removed by nitrogen stripping, and the solution was concentrated by continuous nitrogen stripping to 5 mL on a 90 °C hotplate, followed by filtration through 0.2 μm filter. The functionalized Pdots dispersion is clear and stable for months without aggregation.

Here, in order to get DB-CN-PPV Pdots with different sizes, the above stock solution was further diluted in mixed solvent THF/water with THF volume fraction of 30, 20 %, respectively, and the diluted mixture solutions have a DB-CN-PPV concentration of 50 μg/mL and a PSMA concentration of 10 μg/mL. We used this diluted mixture solution as the starting organic solution, and followed the same procedures. Finally, we obtained DB-CN-PPV Pdots with different sizes.

The DB-CN-PPV/PFBT Pdots were also prepared with same procedures. PFBT was dissolved in pure THF to prepare a stock solution with a concentration of 1 mg/mL. And then, the three polymer solutions (DB-CN-PPV, PFBT, and PSMA) were mixed in pure THF with a DB-CN-PPV concentration of 25 μg/mL, a PFBT concentration of 25 μg/mL, and a PSMA concentration of 10 μg/mL. We used this mixture solution as the starting organic solution, and followed the same procedures. Finally, we obtained DB-CN-PPV/PFBT Pdots.

Biomolecule conjugation

The DB-CN-PPV Pdots bioconjugation were prepared by utilizing the EDC-catalyzed reaction between carboxyl

groups on Pdots surface and amine groups on biomolecules. Typically, 20 μL of poly(ethylene glycol) (5 % wv PEG, MW 3350) and 20 μL of concentrated HEPES buffer (1 M, pH 7.3) were added to 1 mL of functionalized Pdots solution. Then, 40 μL of streptavidin was added to the solution and mixed well on a vortex. 20 μL of freshly prepared solution of EDC (5 mg/mL in water) was added into the solution and mixed by vortex. The mixture was stirred for 4 h at room temperature. Finally, the resulting DB-CN-PPV-streptavidin bioconjugates were separated from free biomolecules by gel filtration using Sephacryl HR-300 gel media.

Cell culture and nanoparticle labeling

Breast cancer cell line MCF-7 cells were ordered from Shanghai Fuxiang Biotechnology Co. Ltd. (Shanghai, China). Cells were cultured in an atmosphere of air/CO_2 (95:5) at 37 °C, using Dulbecco's modified Eagle Medium (DMEM) with 10 % Fetal Bovine Serum (FBS), 50 U/mL penicillin, and 50 μg/mL streptomycin. For labeling the surface marker EpCAM, MCF-7 cells were harvested from the culture flask, washed, centrifuged, and resuspended in a labeling buffer (1 × PBS, 1 % BSA). The MCF-7 cells were dispersed in 100 μL of labeling buffer in a 5 mL round-bottom tube, and sequentially incubated with a biotinylated primary anti-EpCAM (0.5 mg/mL) and DB-CN-PPV-streptavidin bioconjugates, and then imaged on a fluorescence microscopy.

Characterization methods

The particle sizes and morphology of DB-CN-PPV Pdots were measured by dynamic light scattering (DLS) and transmission electron microscopy (TEM). DLS is performed using a 1 cm disposable polystyrene cuvette at 25 °C by Malvern Nano ZEN-3600 instrument, and the TEM images were obtained by a Hitachi H-600 microscope operated at 100 kV. UV–Vis absorption spectra were recorded with a Schimadzu UV-2550 scanning spectrophotometer using 1 cm glass cuvette. Fluorescence spectra were obtained using a Hitachi F-4500 fluorescence spectrophotometer, and the quantum yield was achieved by the relative method and a fluorescent Qdots, Qdots655, as the reference. Single-particle imaging and fluorescent tracer were performed by custom built total internal reflection fluorescence (TIRF) microscope. A 405 nm Sapphire laser beam (Coherent, USA) was directed into an inverted microscope (Olympus IX71, Japan) using steering optical lenses. The objective used for illumination and light collection was a 1.49 NA 100 × TIRF objective (Olympus, Japan). Laser excitation power was measured at the nosepiece before the objective. Fluorescence signal was filtered by a 405 nm long pass filter and imaged on an Andor iXon3 frame transfer EMCCD (Andor Technology, UK). Fluorescent samples were diluted in Milli-Q water, dried under vacuum on cleaned glass coverslips, and imaged on the TIRF microscope. Fluorescence intensity emitted per frame for a given particle was estimated by integrating the CCD signal over the fluorescence spot.

Results and discussion

DB-CN-PPV Pdots, have been prepared by the reprecipitation method, which we have described previously (as shown in Fig. 1) [26, 27]. Briefly, we blended PSMA with DB-CN-PPV during Pdots formation to introduce carboxyl groups on the Pdots surface after the maleic anhydride groups were spontaneously hydrolyzed in aqueous solution (Fig. 1) [28]. The aqueous DB-CN-PPV Pdots are stable and clear (not turbid) for months without aggregation. The sizes of the DB-CN-PPV Pdots were characterized by DLS (Fig. 2a) and TEM (Fig. 2d). The DB-CN-PPV Pdots exhibit a hydrodynamic diameter of ~20 nm, which is consistent with the result of TEM. The carboxyl functionalization did not cause any noticeable change in the particle size. The TEM images also indicate morphologies of DB-CN-PPV particles are spherical as previously reported, because the surface tension effects determine equilibrium shape for conjugated polymer nanoparticles tending to be spherical in this size.

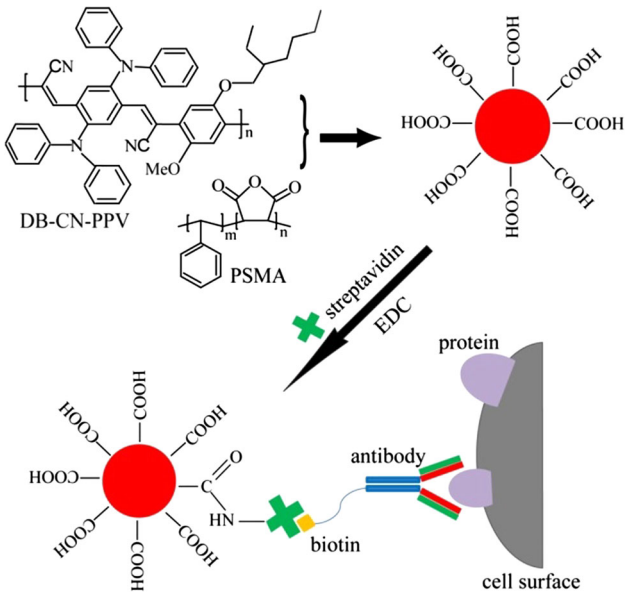

Fig. 1 Schematic illustration of surface functionalization of Pdots and subsequent streptavidin bioconjugation via EDC-catalyzed coupling for specific cellular targeting

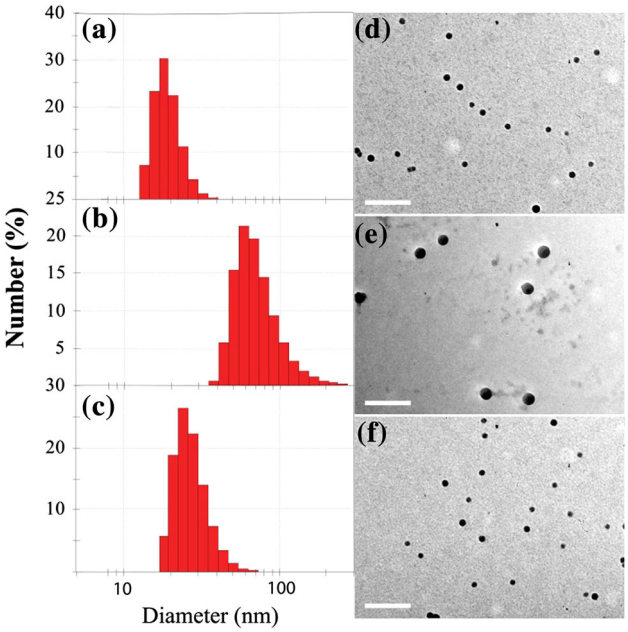

Fig. 2 Configuration of the Pdots: **a**, **b**, **c** DLS results of the Pdots acquired by reprecipitation method. From *top to bottom* show the DLS data of 100 % THF, 30 % THF, and 20 % THF in the polymer mixture solution, respectively; **d**, **e**, **f** typical TEM images of Pdots. From *top to bottom* show the TEM data of 100 % THF, 30 % THF, and 20 % THF in the polymer mixture solution, respectively. The *scale bar* represents 200 nm

In previous study, Wu group investigated CN-PPV Pdots size-dependent fluorescence properties [29]. The results exhibit that the specific size distribution is dependent on the polymer species such as their molecular weight and backbone rigidity. Moreover, the preparation method for different-sized particles has to be optimized for each polymer on a case-by-case basis. So that, we attempt to prepare different-sized DB-CN-PPV Pdots together with controlled chain folding behavior in this study. To obtain DB-CN-PPV Pdots with different sizes, the polymer stock solution was further diluted in mixed solvent THF/water with THF volume fraction of 30, 20 %, respectively, and the diluted mixture solutions have a DB-CN-PPV concentration of 50 μg/mL and a PSMA concentration of 10 μg/mL. The slight decrease of solvent quality may result in the formation of small polymer aggregates with relatively extended chain conformation in the solution. Further this mixture solution was injected into water can produce polymer nanoparticles with relative large sizes and maintain their extended chain conformation. DB-CN-PPV nanoparticles of three different sizes were prepared using reprecipitation approach. As indicated by DLS measurements, an average particle size of 20 nm (Fig. 2a) is determined for the DB-CN-PPV Pdots prepared in pure THF. With the same experimental conditions but increasing water fraction in the mixture solutions, the resulting Pdots show increased particle size, ~59 nm (Fig. 2b) for those prepared in THF/water (3/7, V/V), and ~28 nm (Fig. 2c) for those prepared in THF/water (1/4, V/V). The particle size and morphology were further characterized by TEM. As shown in Fig. 2d, e, f, the TEM images show comparable particle size and distribution the lateral size of the collapsed particle from TEM is largely consistent with the hydrodynamic size from DLS. These results indicate the Pdots size can be successfully controlled by increasing the water content in the mixture solution.

Through the DB-CN-PPV Pdots have different particle sizes, they did not show the size-dependent fluorescence properties. In order to study the spectroscopic properties of Pdots, a Qdots (Qdots655), with similar absorption and emission spectra, are introduced. Figure 3a shows the absorption and emission spectra of the DB-CN-PPV Pdots (prepared from pure THF) and Qdots655 dots in toluene. The DB-CN-PPV Pdots can be conveniently excited by the 360 nm line of a UV laser, and under the same excited line, the Qdots655 dots also gave a sharp peak emission at the same wavelength range. Fluorescence quantum yield measurements indicate that these Pdots exhibit a red-fluorescence quantum with yield of ~27 %. As we know, the available excited line used in cell imaging is visible light [30, 31]. In order to get a good emission peak by visible light excited, we mixed another semiconducting

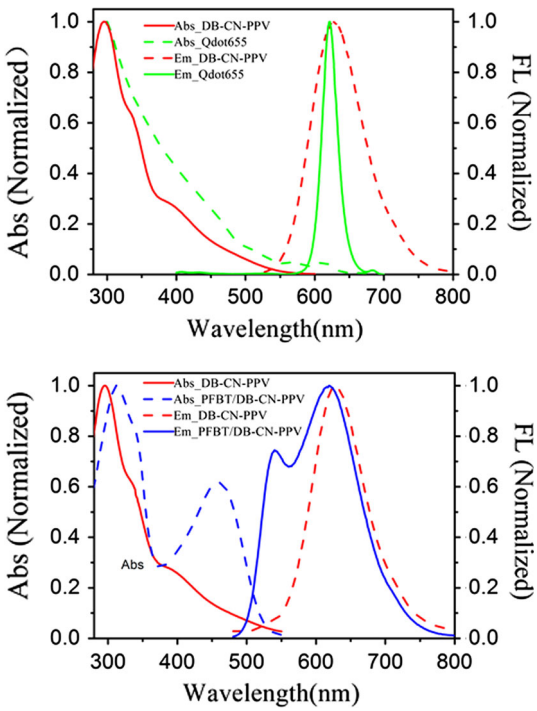

Fig. 3 **a** Absorption and emission spectra of DB-CN-PPV Pdots and Qdots655 *dots* in water; **b** absorption and emission spectra of DB-CN-PPV Pdots and DB-CN-PPV/PFBT mixed Pdots (the mixed molar ratio of 1/1)

polymer PFBT with DB-CN-PPV to get DB-CN-PPV/PFBT Pdots (the mixed molar ration of 1/1), which has good absorption at visible light wavelength range. In order to avoid the effect of particle size, we used same particle size to measure the absorption and emission spectra of DB-CN-PPV/PFBT mixed Pdots and DB-CN-PPV Pdots. The absorption and emission spectra of the DB-CN-PPV/PFBT Pdots are shown in Fig. 3b. From the absorption spectra, the maximum absorption peak is shifted from 295 to 312 nm, and there is a new absorption peak at 460 nm which is the contribution of PFBT. DB-CN-PPV/PFBT Pdots can be excited by the 460 nm line of a blue laser conveniently, matching well with most instruments currently available for biological imaging or flow cytometry. Excited under the 460 nm, the maximum emission peak of DB-CN-PPV/PFBT Pdots is shifted from 629 to 617 nm, closed to the pure red light centre. These results show that the fluorescence properties of DB-CN-PPV Pdots can be tuned by other semiconducting polymer.

An available estimate of fluorescence brightness is determined by spectrum absorption cross-section and the fluorescence quantum yield. In order to compare the brightness of Qdots655 dots and DB-CN-PPV Pdots (prepared in pure THF), single-particle fluorescence imaging was used. As shown in Fig. 4a and b, DB-CN-PPV Pdots exhibit an obvious improvement in signal-to-background ratio compared to Qdots655 dots under 405 nm laser exciting. Intensity histograms were obtained by statistical analyses of hundreds of particles in single-particle images. As shown in the intensity histograms (Fig. 4c, d), the measured average fluorescence brightness of DB-CN-PPV Pdots is about 4 times higher than that of Qdots655 dots. Though the emission peak of DB-CN-PPV Pdots is not a sharp peak (Fig. 3a), DB-CN-PPV Pdots are brighter than Qdots655 dots, owing to a number of favorable characteristics of conjugated polymer molecules, including their high absorption cross sections (typically 10^{-15}–10^{-14} cm^2), high radiative rates, high effective chromophore density, and minimal levels of aggregation-induced fluorescence quenching [20, 32, 33].

The DB-CN-PPV Pdots were employed to investigate on cellular labeling in cultured mammalian cells. As reported previously, based on the combined effect of the surface charge, functionalization, and surface-to-volume ratio related to particle diameters, the favored size of the Pdots used in the cellular labeling is the medium-sized Pdots [34]. So that, the DB-CN-PPV Pdots with diameter 20 nm were used to perform the cellular labeling experiment. The PSMA functionalization generates surface carboxyl groups, and streptavidin can be covalently conjugated to the Pdots by a protocol described before [35]. Zeta potentials were conducted to examine the specific binding of the Pdot-streptavidin bioconjugates. After biomolecule conjugation, the Zeta potentials of the DB-CN-PPV Pdots and DB-CN-

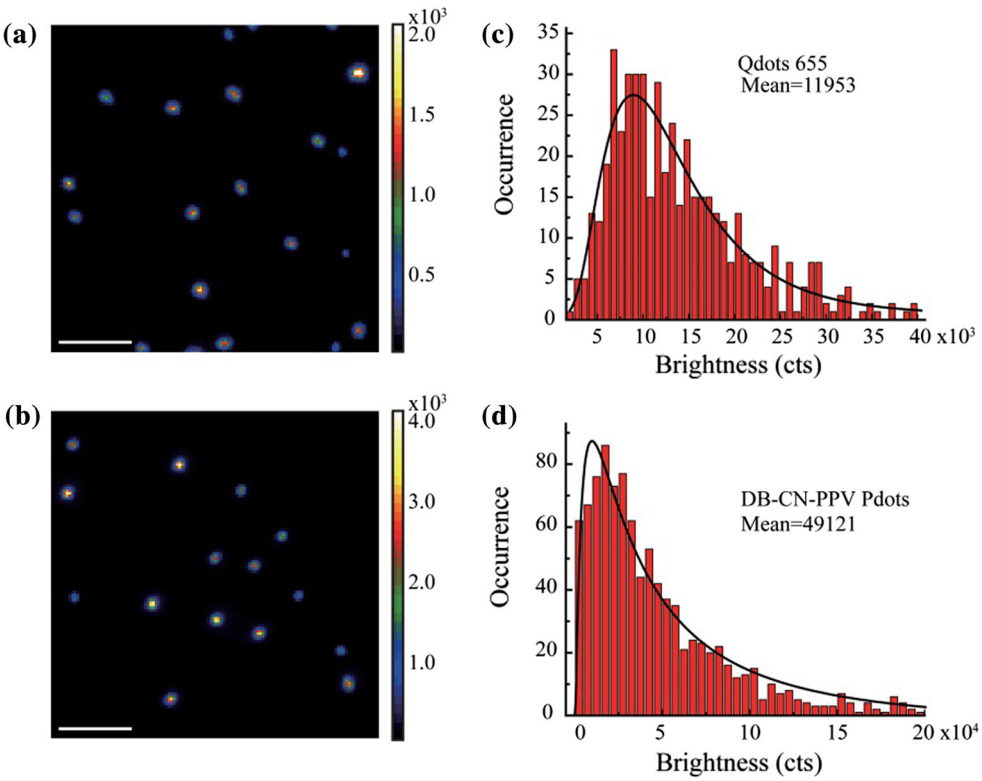

Fig. 4 Single-particle brightness of **a** Qdots655 dots and **b** DB-CN-PPV Pdots immobilized on a glass coverslip, obtained under same excitation and detection conditions; Intensity histograms of **c** Qdots655 dots and **d** DB-CN-PPV Pdots, by analyzing single-particle brightness of hundreds of nanoparticles. The *blue curves* were obtained by fitting a log-normal distribution to the histogram, resulting in average intensities of 11953 and 49121 counts for the two types of *dots*, respectively. *Scale bar* represents 5 μm (Color figure online)

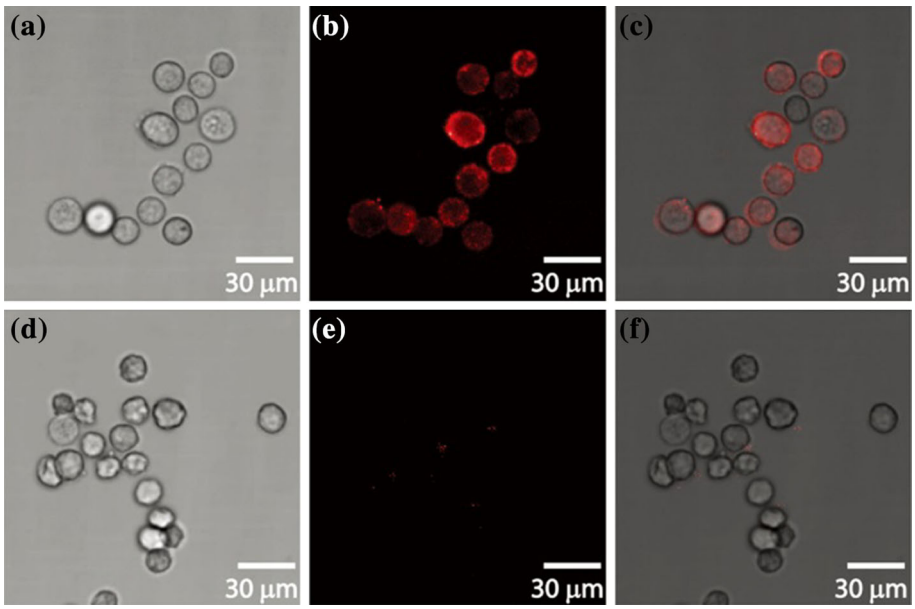

Fig. 5 Fluorescence imaging of cell surface marker (EpCAM) in human breast cancer cells (MCF-7) labeled with DB-CN-PPV-streptavidin bioconjugates. MCF-7 cells were incubated sequentially with biotinylated primary anti-EpCAM antibody and DB-CN-PPV-streptavidin bioconjugates: **a** bright-field images; **b** fluorescence images; **c** combined bright-field and fluorescence image. The cells were incubated in absence of primary antibody as control experiments; **d** bright-field images of control experiments; **e** fluorescence images of control experiments; **f** combined bright-field and fluorescence image of control experiments. *Scale bar* represents 30 μm

PPV-streptavidin bioconjugates were −45.9 and −15.9 mV, respectively, which indicated that the DB-CN-PPV Pdots have been conjugated with streptavidin. Then, the Pdot-streptavidin bioconjugates were used to label a specific cellular target, EpCAM, an epithelial cell-surface marker currently used for the detection of circulating tumor cells [36, 37]. A biotinylated primary anti-EpCAM antibody and the Pdot-streptavidin probes were sequentially incubated with MCF-7 cells. Through the max absorption of the DB-CN-PPV Pdots at UV light region, they also have absorption at visible light region (Fig. 3a) and they can be excited by blue light. Figure 5 shows fluorescence images of the DB-CN-PPV-streptavidin bioconjugates labeling cells as well as the control experiments. Strong fluorescence was observed on the cell surface compared to the control sample (identical conditions but without the primary antibody). These images indicate a staining pattern consistent with perinuclear labeling and brightly fluorescent vacuoles and organelles (e.g., pinosomes and lysosomes). The mechanism of cellular uptake of these fluorescent Pdots have been systematically investigated in a previous report [38, 39], in which temperature-dependent uptake, co-localization study, and inhibition of uptake by phosphoinositide 3-kinase inhibitors indicate macropinocytosis as the operative endocytic mechanism. These evidences demonstrate that the DB-CN-PPV-streptavidin bioconjugates are highly specific for the target. This experiment expands the kind of Pdots application in cellular imaging and biological assays.

Conclusions

In conclusion, we report a new Pdots that is extremely red light bright emission. It spectrally complements existing Pdots because the emission light in the red wavelength range with high brightness and high quantum yield. The Pdots size can be controlled by increasing the water content in the polymer mixture solution. Furthermore, the excited line of the DB-CN-PPV Pdots can be excited by visible light through mixed with the PFBT. In addition, the DB-CN-PPV Pdots show noticeable specific binding during sub-cellular imaging. The adjustable particle size, tunable fluorescence properties, high brightness, and the ability to highly specifically target sub-cellular structures make the DB-CN-PPV Pdots as promising probes for biological imaging and bioanalytical applications.

Acknowledgements This research is supported by National Science Foundation of China (Grants 61222508, 61335001, 21471067, 51302103, and 51402121), Jilin Provincial Science & Technology Department (20140520101JH and 20140520163JH), and SRG2013-00035-FHS Grant, MYRG2014-00093-FHS Grant from University of Macau in Macau and FDCT 026/2014/A1 grant from Macao Government.

References

1. Wu C, Bull B, Szymanski C et al (2008) Multicolor conjugated polymer dots for biological fluorescence imaging. ACS Nano 2:2415–2423

2. Fass L (2008) Imaging and cancer: a review. Mol Oncol 2:115–152
3. Giepmans BN, Adams SR, Ellisman MH et al (2006) The fluorescent toolbox for assessing protein location and function. Science 312:217–224
4. Kobayashi H, Ogawa M, Alford R et al (2009) New strategies for fluorescent probe design in medical diagnostic imaging. Chem Rev 110:2620–2640
5. Vu TQ, Lam WY, Hatch EW et al (2015) Quantum dots for quantitative imaging: from single molecules to tissue. Cell Tissue Res 360:71–86. doi:10.1007/s00441-014-2087-2
6. Thambidurai M, Muthukumarasamy N, Agilan S et al (2010) Strong quantum confinement effect in nanocrystalline CdS. J Mater Sci 45:3254–3258. doi:10.1007/s10853-010-4333-7
7. Wang Q, Seo D-K (2008) Preparation of photostable quantum dot-polystyrene microbeads through covalent organosilane coupling of CdSe@Zns quantum dots. J Mater Sci 44:816–820. doi:10.1007/s10853-008-3138-4
8. Prasad KP, Chen Y, Sk MA et al (2014) Fluorescent quantum dots derived from PEDOT and their applications in optical imaging and sensing. Mater Horiz 1:529–534
9. Derfus AM, Chan WC, Bhatia SN (2004) Probing the cytotoxicity of semiconductor quantum dots. Nano Lett 4:11–18
10. Xu H, Chen C, He Y et al (2015) Analysis of cancer marker in tissues with Hadamard transform fluorescence spectral microscopic imaging. J Fluoresc 25:397–402. doi:10.1007/s10895-015-1525-1
11. Geng J, Li K, Qin W et al (2014) Red-emissive chemiluminescent nanoparticles with aggregation-induced emission characteristics for in vivo hydrogen peroxide imaging. Part Part Syst Charact 31:1238–1243
12. Sun H, Zhang F, Wei H et al (2013) The effects of composition and surface chemistry on the toxicity of quantum dots. J Mater Chem B 1:6485
13. Ye F, Wu C, Jin Y et al (2012) A compact and highly fluorescent orange-emitting polymer dot for specific subcellular imaging. Chem Commun 48:1778–1780
14. Li Q, Zhang J, Sun W et al (2014) Europium-complex-grafted polymer dots for amplified quenching and cellular imaging applications. Langmuir 30:8607–8614
15. Feng G, Li K, Liu J et al (2014) Bright single-chain conjugated polymer dots embedded nanoparticles for long-term cell tracing and imaging. Small 10:1212–1219
16. Wu C, Szymanski C, McNeill J (2006) Preparation and encapsulation of highly fluorescent conjugated polymer nanoparticles. Langmuir 22:2956–2960
17. Joshi PB, Zhang P (2015) Facile capture of conjugated polymer nanodots in silica nanoparticles to facilitate surface modification. J Mater Sci 50:3597–3603. doi:10.1007/s10853-015-8920-5
18. Huang Y-C, Chen C-P, Wu P-J et al (2014) Coumarin dye-embedded semiconducting polymer dots for ratiometric sensing of fluoride ions in aqueous solution and bio-imaging in cells. J Mater Chem B 2:6188
19. Wu C, Schneider T, Zeigler M et al (2010) Bioconjugation of ultrabright semiconducting polymer dots for specific cellular targeting. J Am Chem Soc 132:15410–15417
20. Yu J, Wu C, Tian Z et al (2012) Tracking of single charge carriers in a conjugated polymer nanoparticle. Nano Lett 12:1300–1306
21. Wu I, Yu J, Ye F et al (2014) Squaraine-based polymer dots with narrow, bright near-infrared fluorescence for biological applications. J Am Chem Soc 137:173–178
22. Junkers T, Vandenbergh J, Adriaensens P et al (2012) Synthesis of poly(p-phenylene vinylene) materials via the precursor routes. Polym Chem 3:275–285
23. Wu C, Szymanski C, Cain Z et al (2007) Conjugated polymer dots for multiphoton fluorescence imaging. J Am Chem Soc 129:12904–12905
24. Adebanjo O, Maharjan PP, Adhikary P et al (2013) Triple junction polymer solar cells. Energy Environ Sci 6:3150–3170
25. Wu C, Hansen SJ, Hou Q et al (2011) Design of highly emissive polymer dot bioconjugates for in vivo tumor targeting. Angew Chem Int Ed 50:3430–3434
26. Wu C, Chiu DT (2013) Highly fluorescent semiconducting polymer dots for biology and medicine. Angew Chem Int Ed 52:3086–3109
27. Chang K, Liu Z, Chen H et al (2014) Conjugated polymer dots for ultra-stable full-color fluorescence patterning. Small 10:4270–4275
28. Wu C, Jin Y, Schneider T et al (2010) Ultrabright and bioorthogonal labeling of cellular targets using semiconducting polymer dots and click chemistry. Angew Chem Int Ed 49:9436–9440
29. Sun K, Chen H, Wang L et al (2014) Size-dependent property and cell labeling of semiconducting polymer dots. ACS Appl Mater Interfaces 6:10802–10812
30. Wu Y, Shi M, Zhao L et al (2014) Visible-light-excited and europium-emissive nanoparticles for highly-luminescent bioimaging in vivo. Biomaterials 35:5830–5839
31. Zhang X, Yu J, Rong Y et al (2013) High-intensity near-ir fluorescence in semiconducting polymer dots achieved by cascade fret strategy. Chem Sci 4:2143–2151
32. Pei Q, Yang Y (1996) Efficient photoluminescence and electroluminescence from a soluble polyfluorene. J Am Chem Soc 118:7416–7417
33. Liu Z, Sun Z, Di W et al (2015) Brightness calibrates particle size in single particle fluorescence imaging. Opt Lett 40:1242–1245
34. He C, Hu Y, Yin L et al (2010) Effects of particle size and surface charge on cellular uptake and biodistribution of polymeric nanoparticles. Biomaterials 31:3657–3666
35. Li Q, Sun K, Chang K et al (2013) Ratiometric luminescent detection of bacterial spores with terbium chelated semiconducting polymer dots. Anal Chem 85:9087–9091
36. Beta M, Khetan V, Chatterjee N et al (2014) EpCAM knockdown alters microRNA expression in retinoblastoma: functional implication of EpCAM regulated miRNA in tumor progression. PLoS One 9:e114800
37. Ligtenberg MJ, Kuiper RP, Geurts van Kessel A et al (2013) EPCAM deletion carriers constitute a unique subgroup of Lynch syndrome patients. Fam Cancer 12:169–174
38. Feng G, Liu J, Zhang R et al (2014) Cell imaging using red fluorescent light-up probes based on an environment-sensitive fluorogen with intramolecular charge transfer characteristics. Chem Commun 50:9497–9500
39. Fernando LP, Kandel PK, Yu J et al (2010) Mechanism of cellular uptake of highly fluorescent conjugated polymer nanoparticles. Biomacromolecules 11:2675–2682